

RSC Advances

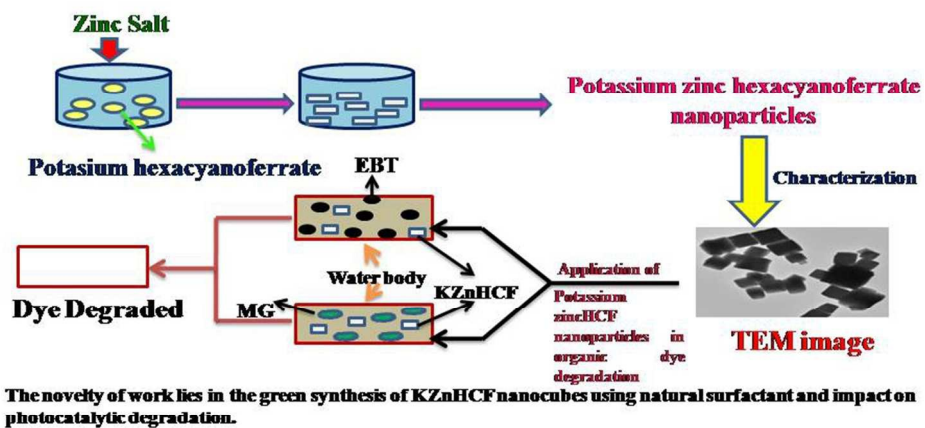


This is an *Accepted Manuscript*, which has been through the Royal Society of Chemistry peer review process and has been accepted for publication.

Accepted Manuscripts are published online shortly after acceptance, before technical editing, formatting and proof reading. Using this free service, authors can make their results available to the community, in citable form, before we publish the edited article. This *Accepted Manuscript* will be replaced by the edited, formatted and paginated article as soon as this is available.

You can find more information about *Accepted Manuscripts* in the [Information for Authors](#).

Please note that technical editing may introduce minor changes to the text and/or graphics, which may alter content. The journal's standard [Terms & Conditions](#) and the [Ethical guidelines](#) still apply. In no event shall the Royal Society of Chemistry be held responsible for any errors or omissions in this *Accepted Manuscript* or any consequences arising from the use of any information it contains.



254x190mm (96 x 96 DPI)

Title of the Paper:

Green Synthesis of potassium zinc hexacyanoferrate nanocubes and its potential application in photocatalytic degradation of organic dyes

Vidhisha Jassal^a, Uma Shanker^{a*} B S Kaith^a and Shiv Shankar^b

jassalvidhisha@gmail.com, shankeru@nitj.ac.in, kaithbs@nitj.ac.in, shiv.nature@gmail.com ,

^aDepartment of Chemistry, Dr B R Ambedkar National Institute of Technology
Jalandhar, Punjab, India-144011

^bDepartment of Environmental Science, Babasaheb Bhimrao Ambedkar University,
Lucknow, India-226025

*** Corresponding Author**

Dr Uma Shanker (Assistant Professor)

CE-306

Dept of Chemistry

Dr B R Ambedkar National Institute of Technology Jalandhar, India-144011

Email: shankeru@nitj.ac.in, umaorganic29@gmail.com

Contact number: +91- 7837-588-158 (Mobile)

+91-0181-269-301-2258

Fax: +91-0181-269-0932

Abstract

A novel green route was used to synthesize potassium zinc hexacyanoferrates ($K_2Zn_3[Fe(CN)_6] \cdot 2.9H_2O$) (KZnHCF) nanocubes using *Sapindus mukorossi* as natural surfactant and water as solvent. The synthesized nanoparticles were characterized by Powder X-ray diffraction (PXRD), Scanning electron microscopy (SEM), Transmission electron microscopy (TEM), Fourier Transform Infrared Spectroscopy (FTIR), Thermogravimetric techniques and BET surface area analysis. KZnHCF nanoparticles were investigated for their effect on photocatalytic degradation of two synthetic dyes namely Eriochrome Black T (EBT) and Malachite Green (MG). The effect of process parameters like pH, temperature, KZnHCF dose and concentration of dye on KZnHCF mediated degradation of both dyes was also investigated. Under optimized conditions, KZnHCF resulted in 94.15% degradation of MG followed by 76.13% EBT degradation.

Keywords: Potassium zinc hexacyanoferrate, Natural biosurfactant (*Sapindus mukorossi*), nanocubes, Eriochrome Black T (EBT), Malachite Green (MG), photocatalytic degradation.

1. Introduction:

Metal hexacyanoferrates (MHCF) with general formula $M_k[Fe(CN)_6] \cdot xH_2O$ represent an important class of coordination compounds, where k represents stoichiometric number [1]. Over the last few decades such compounds have gained attraction all over the world because of their peculiar physicochemical properties like electrochromism [2,3], photo electrochromism [4], energy storage [5,6], electrolytic and sensing properties [1,7] through molecular architecture.

ZnHCF differs from other Prussian blue (PB) analogues because of certain unique properties like Zn has completely filled 3d as well as 4s orbitals and narrow band gap. Moreover, ZnHCF can be formed only in a certain ratio of the modification species. Electrocrystallization phenomenon has been found to be predominant over stable surface modification [8]. ZnHCF is a unique exception as it does not get deposited easily on surfaces like glassy carbon (GC), Pt and Au [8,9, 10].

Because of shape and size dependent properties of ZnHCF nanoparticles, their use as a semiconductor in the photocatalytic degradation of various harmful dyes has drawn the attention of Scientific fraternity for the applications of such nano-coordination compounds in the treatment of textile and other related industrial effluents.

Synthetic dyes are extensively used in the textile industries and as per report worldwide 2,80,000 tons of textile dyes are discharged in industrial effluents every year [11]. Discharge of untreated effluents under anaerobic conditions causes formation of toxic aromatic amines in receiving water bodies. Since synthetic dyes are toxic, mutagenic and carcinogenic [12] and increase the COD, therefore, efficient removal of dyes from industrial effluents is a major environmental challenge [13,14].

Malachite green (MG) a water soluble synthetic textile dye [17] because of its toxic effects has become one of the most controversial dyes [18, 19]. It provides undesirable color to the water bodies and reduces sunlight penetration, thereby effecting the lives of several aquatic species [20,21]. On the other hand, anionic Eriochrome Black T (EBT) has the share of more than 50% of the global dye production [22]. Its complex molecular structure and resistance to light, water and chemicals is one of the major environmental problem [22,23].

During last few decades development of clean and efficient water purification technology has been the focus of research. Nanoparticle mediated heterogeneous photodegradation has

emerged as one of the most powerful methods of water decontamination because of its potential to transform recalcitrant organic contaminants into mineral salts and relatively innocuous end products like CO₂ and H₂O [1, 15, 16].

Moreover, natural non-ionic biosurfactants are emerging as eco-friendly and efficient materials for the synthesis of nanoparticles [24,25,26]. Saponins, one of the most commonly used biosurfactants is largely found in plants like *Sapindus mukorossi*, Quillaja bark [27], soyabean [28] and *Fagonia indica* [29]. Rithanuts obtained from the trees of *Sapindus mukorossi* in its powdered state is one of the major ingredients in the herbal products like fabric washings, bath soaps, shampoos, hair dyes and body-care lotions [30].

At critical micellar concentration such bio-surfactants tend to form micelles and assist in the synthesis of different types of nano-structures. *Sapindus mukorossi* belongs to the plant family Sapindaceae and order Sapindeae. Nut powder of this plant is non-ionic natural biosurfactant which contains about 6 to 10 wt% of Saponin [31]. Saponins are widely used in pharmaceuticals [32, 33], detergents [34] and environmental remediation [35].

In present study, a novel eco-friendly method for the synthesis of potassium zinc hexacyanoferrate nanocubes was developed using bio-surfactant. To the best of our knowledge, so far no studies have been reported using *Sapindus mukorossi* (raw ritha) as a natural surfactant for the synthesis of zinc hexacyanoferrate nanoparticles. The effect of potassium zinc hexacyanoferrates on photocatalytic degradation of Malachite green (MG) and Eriochrome Black T (EBT) was investigated. The process parameters favoring maximum degradation of these two synthetic dyes were also optimized.

2. Experimental details

2.1 Materials: All reagents used in the study were of analytical grade. Potassium hexacyanoferrate (II), zinc salt, Eriochrome Black T and Malachite Green were purchased from Merck, India Ltd. *Sapindus mukorossi* was purchased from Jalandhar city, Punjab India.

2.2 Synthesis of potassium zinc hexacyanoferrate nanoparticles:

Bio-surfactants are surface active agents produced by plants or microorganisms. Using the same mechanism as chemical surfactants, they are able to reduce the surface and interfacial tension, thereby reducing the size of the particles. They have several unique features which makes them a promising alternative to chemically synthesized surfactants. These include stable activity at extreme pH, higher biodegradability than chemical surfactants which remains

as such, thus leading to environmental pollution. So, these bio-surfactants are eco-friendly. Also, they have negligible toxicity. On the other hand, most of the chemical surfactants are produced by petroleum feed stocks, hence more toxic and less biodegradable. Since the bio-surfactants like *sapindus mukorossi* used by authors, are biodegradable and have negligible toxic effect on the environment, thus the synthesis of KZnHCF nanocubes employing *sapindus mukorossi* can be called as ‘green synthesis’.

Here, we report the green synthesis of potassium zinc hexacyanoferrate nanoparticles using *Sapindus mukorossias* a biosurfactant. 100 ml solution of 0.1M potassium hexacyanoferrate (II) containing an equimolar amount of potassium chloride was slowly added to a 100 ml solution of 0.1M ZnCl₂ containing an equimolar amount of *Sapindus mukorossi* with constant stirring. An excess of metal salt was used to improve the coagulation of the precipitate. The reaction mixture was heated at 60 °C on water bath for 2–3 hours and finally kept undisturbed for 24 hours at ambient temperature. The precipitates were filtered, washed thoroughly with double distilled water and dried in oven at 60 °C.

2.3 Characterization

The synthesized nanoparticles were characterized using various techniques like Powder X-ray diffraction (PXRD) which was recorded with a P analytical Xpert Pro spectrometer using Cu K α_1 radiation (wavelength 1.540 Å). In order to investigate the surface morphology and average particle size of the synthesized nanoparticles, Scanning electron microscopy (SEM) was carried out. The elemental composition was determined using Energy dispersed spectroscopy (EDS). Transmission electron microscopy (TEM) gave information regarding exact particle size and shape of the nanoparticles. Fourier transform infrared spectroscopy (FT-IR) was also performed to understand the bonding present in the coordination complex. The BET (Brunauer -Emmett –Teller) surface area measurement was done using a BET N₂-physisorption instrument (Nova Station A, Quantachrome Nova Win instrument, version 10.01). The N₂ adsorption was measured at 77.3 K with the assumption of cross-sectional area of N₂ 16.2 (Å)² and liquid density as 0.808g/cc.

2.4 Photocatalytic degradation

Photodegradation experiments were performed with a photocatalytic reactor system to degrade MG and EBT. The bench-scale system is a cylindrical Pyrex-glass cell with 1.0 L

capacity, 10 cm inside diameter and 15 cm height. Irradiation experiments were performed using medium pressure Hg lamp. A magnetic stirrer was used continuously to guarantee good mixing of the solution. The aliquot was taken out at different time intervals. To check the catalytic activity of $K_2Zn_3[Fe(CN)_6]_2 \cdot 9H_2O$ nanocubes different parameters such as catalyst concentration, initial concentration of dye, initial pH and temperature of the dye solution were investigated. The absorption spectra of the dye solutions were recorded using Agilent Pro spectrometer and the rate of degradation was observed at different time intervals in terms of change of intensity at λ_{max} i.e 615-619 nm (MG) and 560 nm (EBT). The dye degradation efficiency (%) has been calculated as:

$$\text{Degradation efficiency(\%)} = \frac{(C_0 - C)}{C_0} \times 100$$

Where C_0 is the initial concentration of dye and C is the concentration of dye after photo-irradiation at particular time interval.

3. Results and discussion:

Chandra *et al.* [36] reported the octahedral geometry of $[Fe(CN)_6]^{4-}$ with six CN^- ligands surrounding the central metal ion. CN^- ligands being strong field ligands will forcefully get paired up the 6 electrons present in the inner sphere of Fe^{2+} and a low-spin t_{2g}^6 configuration is achieved. Moreover, there is a significant back-bonding between the metal $d\pi$ orbitals to the antibonding $p\pi$ orbitals of the CN^- ligands. The outer sphere metal Zn metal is coordinated to the Nitrogen end of the cyanide ligand present inside the $[Fe(CN)_6]^{4-}$ anionic sphere.

Powder X-ray diffraction measurements (Powder Method, Analytical X.Pert Pro) were carried out (Figure 1). Interplanar spacing and the relative intensity data were found in good agreement with the JCPDS values (JCPDS card No 33-1061). The clear and sharp X-ray peaks indicated the high crystallinity of synthesized nanomaterial.

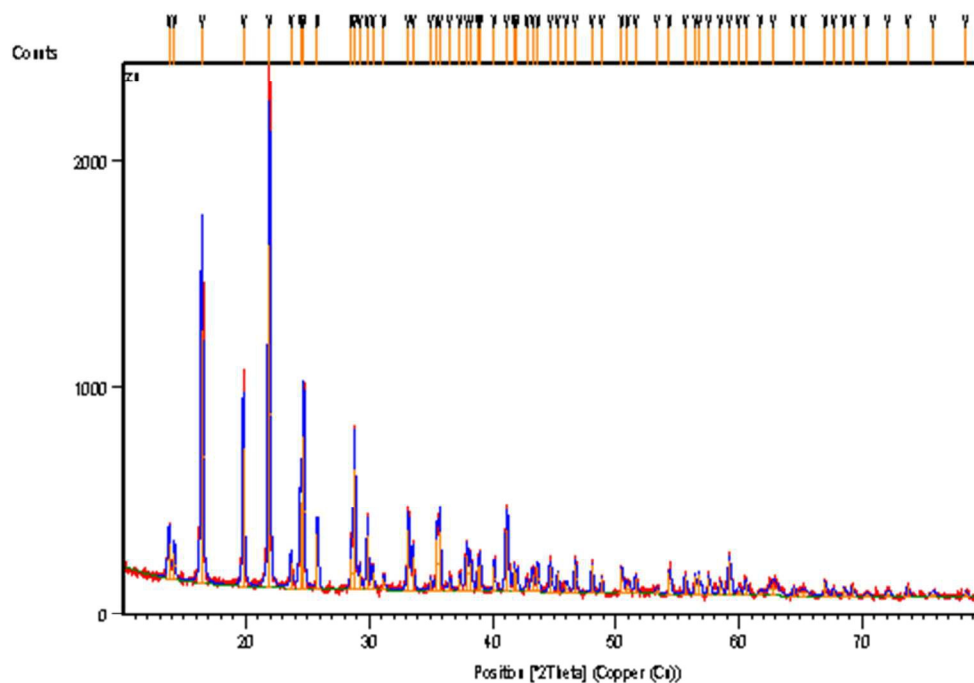
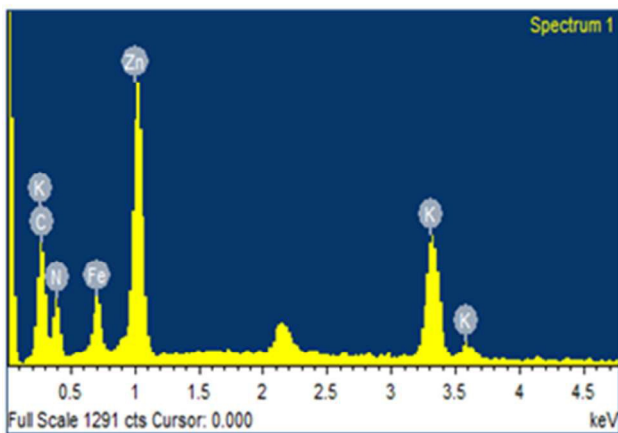
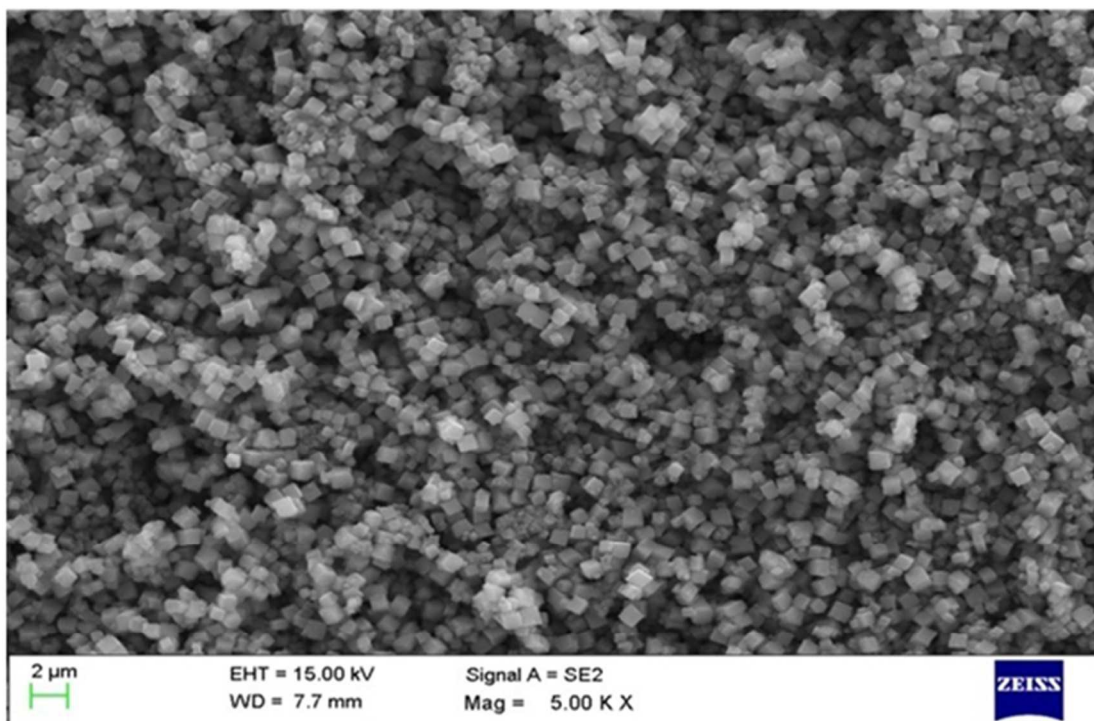


Figure 1: XRD pattern of $K_2Zn_3[Fe(CN)_6]_2 \cdot 9H_2O$

The surface morphology of Potassium zinc hexacyanoferrate nanostructures was evaluated by field emission scanning electron microscopy (FESEM, QUANTA 200 FEG) which revealed that the synthesized products were monodispersed nanocubes with size ranging from 33 to 192 nm (Figure 2), however, slightly agglomerated particles were observed during its morphological investigations. To examine the elemental composition, the synthesized nanocubes were analyzed by energy dispersive spectroscopy (EDS) which showed the presence of Zn, Fe, N, C and K with atomic percentage 8.32%, 5.83%, 41.03%, 39.93% and 4.89%, respectively.



Element	Atomic percentage (%)
C	39.93
N	41.03
Fe	5.83
K	4.89
Zn	8.32
Total	100

Figure 2: FE-SEM image with Elemental composition (EDS) pattern of $K_2Zn_3[Fe(CN)_6]_2 \cdot 9H_2O$ nanocubes

To investigate the exact size and shape of synthesized potassium zinc hexacyanoferrate nanoparticles TEM (Hitachi, H-7500) was employed (Figure 3). Interestingly, potassium zinc hexacyanoferrates have been found to be consisting of the uniform monodisperse cubic shape nanostructures with size ranging around 100 nm. Morphology was clear and well dispersed

with sharp nanocubes. However, slight agglomeration was also observed among the cubical nanoparticles.

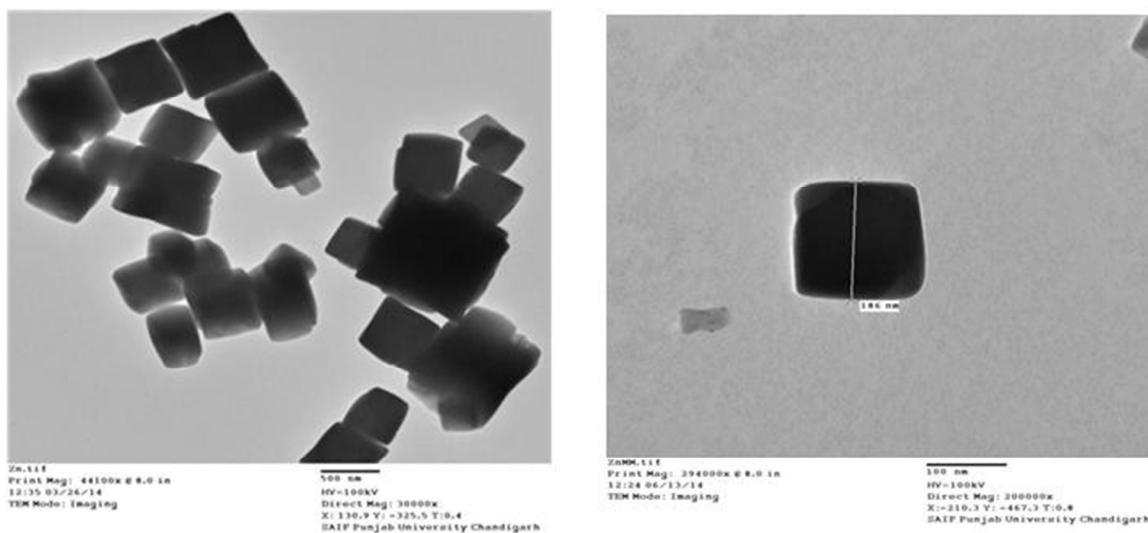


Figure 3: TEM images of $K_2Zn_3[Fe(CN)_6]_2 \cdot 9H_2O$ nanocubes

FT-IR studies were also carried out (Figure 4) to determine the various functional groups present in the synthesized products. It is well known that the single, broad band of the ν_{CN} absorption of PB-structured materials in the range of $2000\text{--}2200\text{ cm}^{-1}$ is diagnostic of the C-bound metal ion and its oxidation state, but is much less sensitive to the N-bound metal ion and its oxidation state. Peak below 400 cm^{-1} corresponds to the metal ion peak. Its frequency varies depending upon the transition metal ion. In case of potassium zinc hexacyanoferrate nanocubes, $C\equiv N$ group present in the species shows a strong peak at 2090 cm^{-1} whereas peak corresponding to Zn-N is observed at 491 cm^{-1} . Also, a broad peak at 3631 cm^{-1} is due to the presence of OH moiety from water molecules. Peak at 1614 cm^{-1} is due to HOH bending. Lastly, peak at 602 cm^{-1} corresponds to Fe-C stretching.

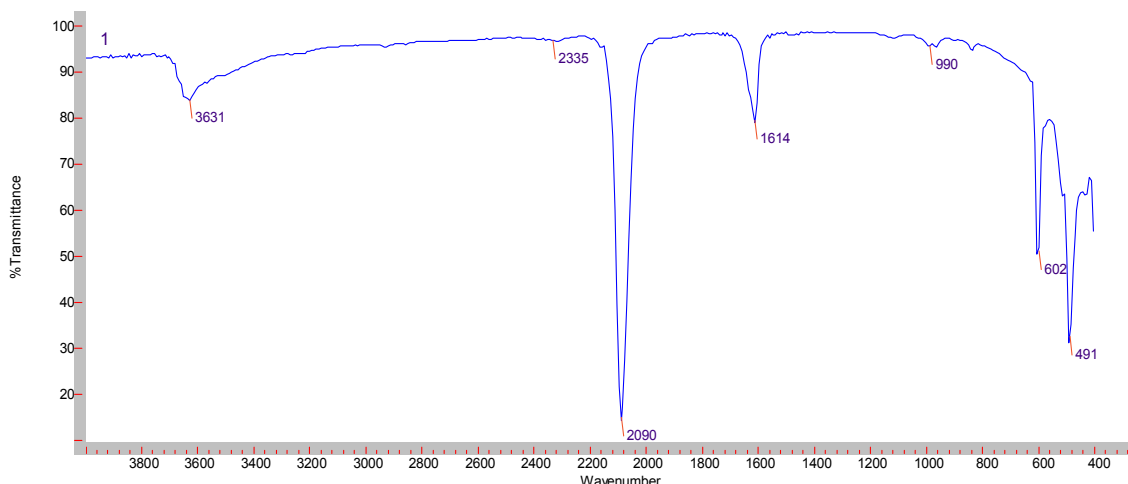


Figure 4: FT-IR spectra of $K_2Zn_3[Fe(CN)_6]_2 \cdot 9H_2O$ nanocubes

Thermal analysis showed that potassium zinc hexacyanoferrate nanoparticles ($K_2Zn_3[Fe(CN)_6]_2 \cdot 9H_2O$) decomposes slowly on heating to $100^\circ C$ and it decomposes at relatively a higher rate from $100^\circ C$ to $203.2^\circ C$. The mass loss was nearly 12.6% upto $203.2^\circ C$. This weight loss could be referred to the loss of water of crystallization. No significant mass loss was observed upto $420^\circ C$, but after that a drastic loss was found when heating the compound from $420^\circ C$ to $734^\circ C$ (nearly 29% wt. loss). The additional loss in weight could be due to the removal of cyanide moiety. Around 40% of the residue remained at the end of the experiment (Figure 5). Possible mechanism could be described as shown below:

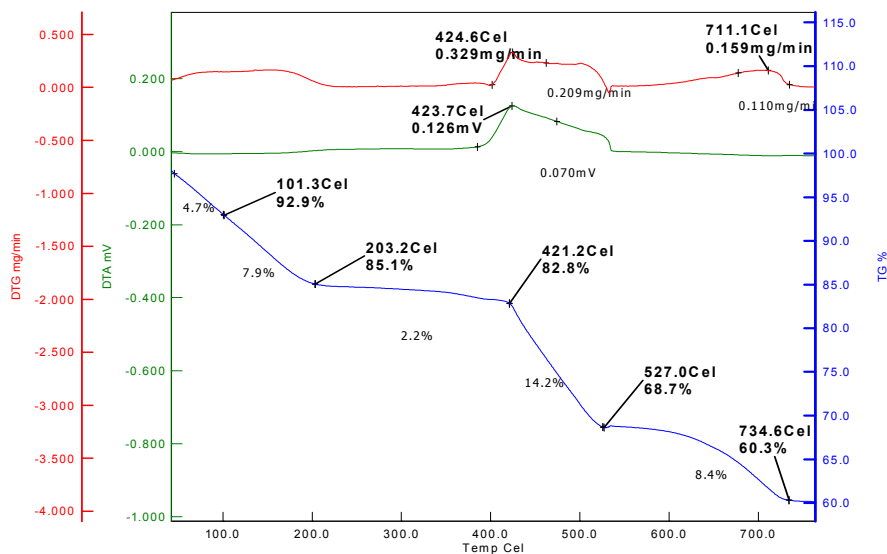


Figure 5: Thermal analysis of $K_2Zn_3[Fe(CN)_6]_2 \cdot 9H_2O$ nanocubes

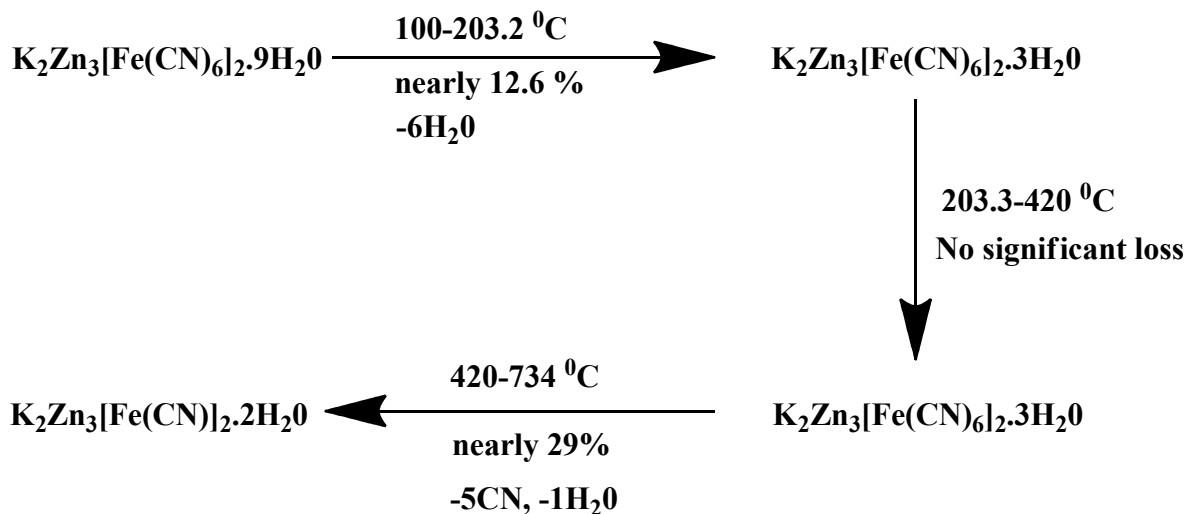


Figure 6: Proposed scheme for the weight loss during TGA

The specific surface area of KZnHCF nanocubes was calculated using the Multi-Point BET surface area analysis technique and was found to be $50.919 \text{ m}^2/\text{g}$. Using this value of surface area, average equivalent particle size can be calculated by using the equation $D_{\text{BET}} = 6000/(\rho \cdot S_w)$, where D_{BET} is the average diameter of the particle (in nm), S_w represents measured surface area of the nanoparticles in m^2/g and ρ is the theoretical density in g/cc . From the above equation, average diameter of the particle was calculated as 145.87 nm , which is in well agreement with the TEM results. The Langmuir surface area, total pore volume and average pore radius was found out to be $72.372 \text{ m}^2/\text{g}$, $4.600 \times 10^{-2} \text{ cc}/\text{g}$ and $1.32317 \times 10^2 \text{ \AA}$, respectively.

Photocatalytic activity

In order to evaluate the photocatalytic effect of potassium zinc hexacyanoferrate nanocubes in the degradation of MG and EBT, measurement of absorbance at regular time intervals was carried out. Two different processes are occurring throughout the reaction on the surface of photocatalyst i.e KZnHCF nanocubes. When the dye solution was exposed to light in the presence of KZnHCF nanocubes, the first step may be dye adsorption on the surface of the catalyst (KZnHCF nanocubes), confirmed by Langmuir adsorption isotherms. Then, catalyst also absorbs the light to excite its electron from valence band to conduction band, thereby leaving behind a hole. The *in situ* generated hole reacts with the water molecules present in

the dye solution and converts it into very reactive hydroxyl free radical (OH^\bullet). These free radicals (OH^\bullet) then reacts with the dye molecules to generate colourless form of the dye, which is ultimately degraded into final colourless products.

Different parameters such as photocatalyst dose, initial concentration of dye, initial pH and temperature of the dye solution were studied for getting the maximum dye degradation. The prime motive behind these choices was to achieve maximum degradation of these two harmful organic dyes i.e. MG and EBT. Since the effluents from dyestuff and textile industries, which are the major sources that release various kinds of dyes into the water bodies, reach water bodies, thus, pH and temperature of water as well as dye concentration is an essential parameter to be investigated. Moreover, amount of catalyst required to degrade these harmful organic dyes is an important criteria. So, the authors decided to investigate the above mentioned four parameters for achieving maximum degradation of MG and EBT dye.

Absorbance was recorded after each interval of 20 minutes and carried out upto 2 hours. Absorbance intensity was found to decrease continuously with increase in time interval and maximum degradation of MG (94.15%) and EBT (76.13%) was observed at 2 hr interval. It may be due to the reason that catalyst used is a semiconductor which upon photo illumination generates electron-hole pairs. The generation of electron-hole pairs is responsible for the photodegradation of MG and EBT. Further the photodegradation of both MG and EBT was found to be initial dye concentration dependent. In both cases maximum photocatalytic degradation was observed at 5ppm concentration. The possible explanation could be at this dye concentration maximum number of active sites on potassium zinc hexacyanoferrate are available for adsorption of dyes. As the concentration increases, the active sites for adsorption present on nanocubes get blocked, thus the rate of dye degradation decreases. In case of temperature dependent dye degradation studies, it was found that with increase in temperature, relative absorption intensity decreased and negligible dye degradation was observed. Thus, potassium zinc hexacyanoferrate nanocubes in case of MG and EBT degradation act as a photocatalyst not thermocatalyst. However, photodegradation of both the dyes was found to be dependent upon the concentration of potassium zinc hexacyanoferrate nanocubes. At the concentration of 15mg of nanocubes per 10 ml of dye solution maximum photodegradation of 94.15% and 76.13% was found in case of MG and EBT, respectively. This could be due to the

reason that at low dye concentration which was optimized earlier, too high and low dose amounts of the catalyst was not a favourable condition. A moderate condition i.e. 15 mg of the catalyst was favoured for the best decomposition of MG and EBT. In case of MG and EBT adsorption and their photocatalytic degradation pH was found to play an important role. Photocatalytic degradation was found to increase with increase in pH. However, maximum adsorption and degradation was found at pH 7. Further increase in pH resulted in decreased dye adsorption and degradation. This could be due to the ion screening effects of H^+ ions under acidic conditions and OH^- ions in alkaline medium. KHCF nanocubes are insoluble in water as well as fairly stable in acids like HCl, HNO_3 , H_2SO_4 as well as bases like NaOH, KOH etc. Thus, after the completion of reaction, catalyst was recovered and used again for similar reactions.

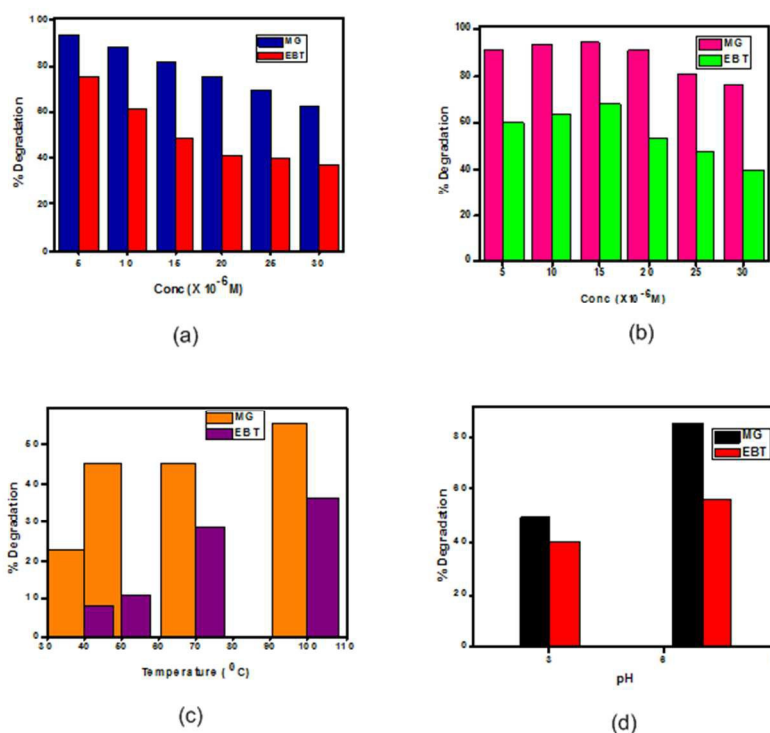


Figure 7: Effects of variation of different parameters on the photocatalytic degradation of EBT and MG dyes.

Reaction mechanism studies

Adsorption isotherm (Figure 8) of MG and EBT in the present case clearly shows that adsorption is fast in both the cases and the isotherms are regular, positive, and concave to the concentration axis. Adsorption data can be represented through a Langmuir adsorption isotherm which assumes the formation of a monolayer of solute molecules on the surface of the adsorbent [37]. A typical graph of C_e/X_e v/s C_e is a straight line (Where C_e Equilibrium concentration of solute in mole/l and X_e amount of solute adsorbed per gram weight of adsorbent (mg) (Figure 9). The adsorption data was fitted in Langmuir adsorption equation:

$$\frac{C_e}{X_e} = \frac{1}{k_L X_m} + \frac{C_e}{X_m}$$

or

$$\frac{1}{X_e} = \frac{1}{C_e} \left(\frac{1}{k_L X_m} \right) + \frac{1}{X_m}$$

Where, C_e is the equilibrium concentration of the dye solution; X_e the amount of dye adsorbed per gram weight of adsorbent; X_m the amount of dye adsorbed at saturation; k_L the langmuir adsorption constant.

k_L and X_m values were determined and shown in Table 1. The X_m values indicate that MG adsorbed more than EBT on potassium zinc hexacyanoferrate nanoparticles. It may be due to more availability of N atoms of MG for interaction with potassium zinc hexacyanoferrate nanoparticles.

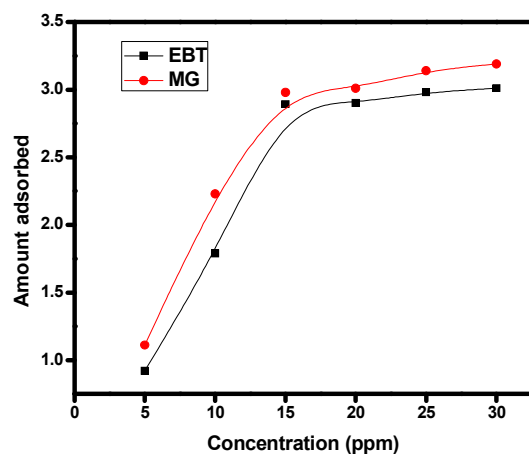


Figure 8: Adsorption isotherm for adsorption of dyes on potassium zinc hexacyanoferrate nanoparticles

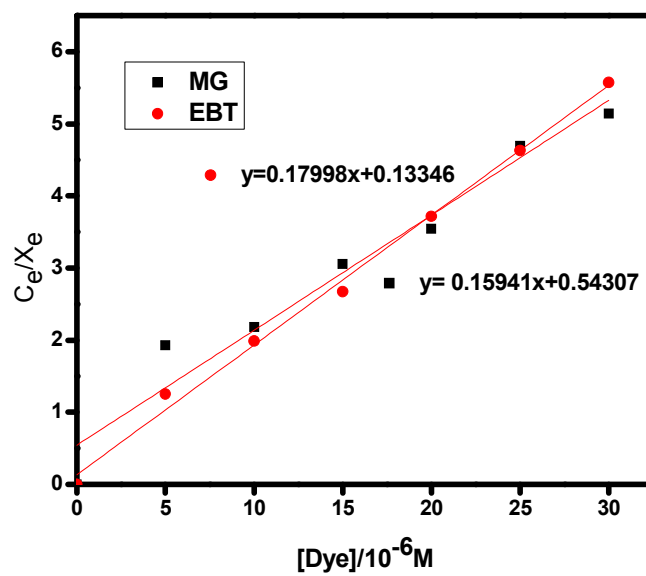


Figure 9: Langmuir isotherms for adsorption of MG and EBT on potassium zinc hexacyanoferrate nanoparticles

Table 2. Langmiur constants for MG and EBT adsorption on potassium zinc hexacyanoferrate nanoparticles

Dye	X_m(mg/g)	K_L(dm³/mol)
MG	6.273	3.406
EBT	5.556	0.7415

From the literature survey it was observed that potassium zinc hexacyanoferrate is semiconducting with a lesser band gap difference [38, 39], so molecular excitation occurs very easily with a light of equal or higher energy than the band gap, thereby generating electrons and holes in between conduction and valence bands. This followed by a series of chemical reactions leading to the formation of hydroxyl radicals. It is the OH[•] which leads to the photodegradation of harmful organic dyes. The following reaction sequence is proposed for the degradation of dyes in presence of KZnHCF nanocubes (Figure 10 and 11):

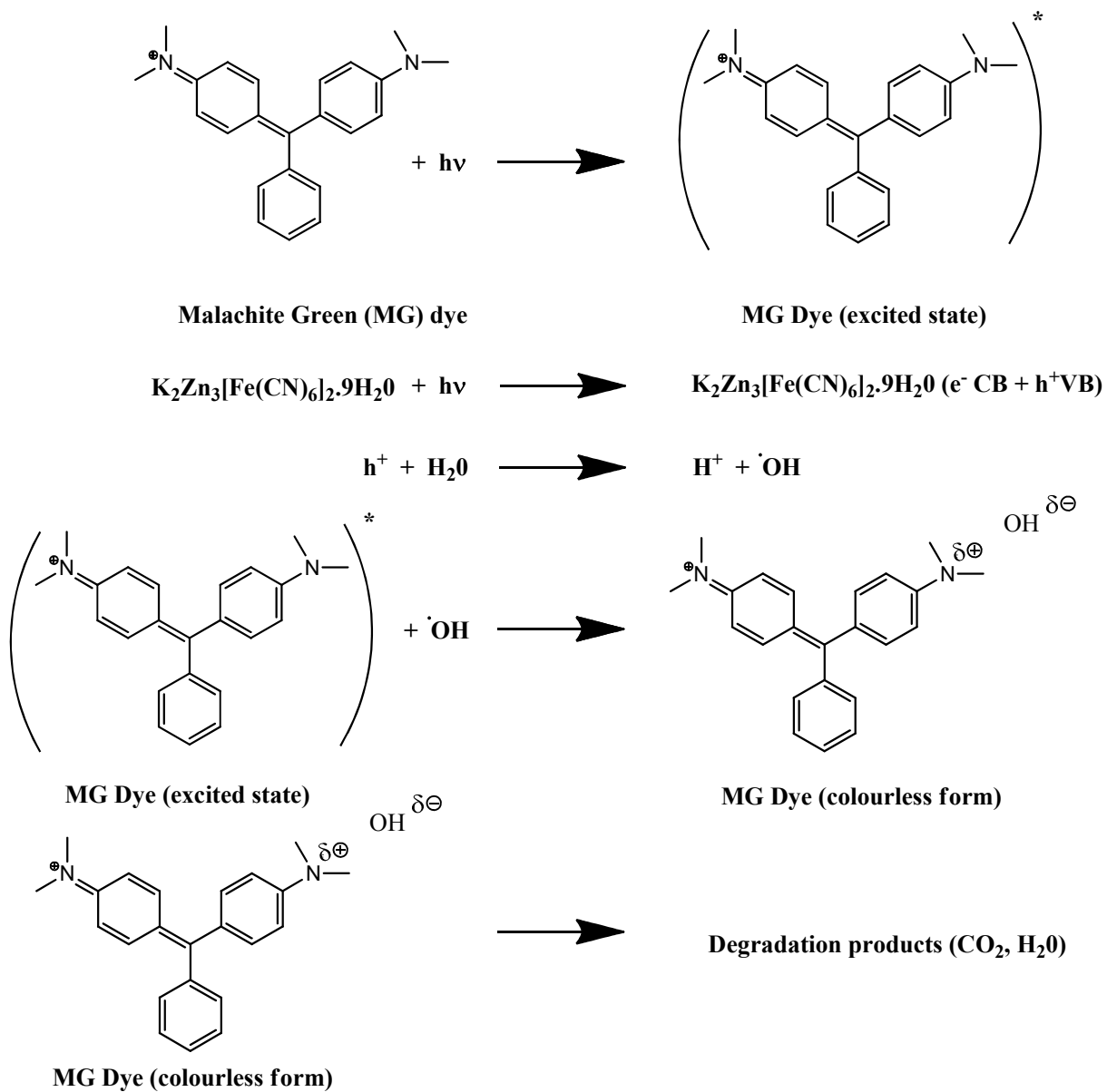


Figure 10: Photocatalytic degradation of MG in presence of KZnHCF nanocubes

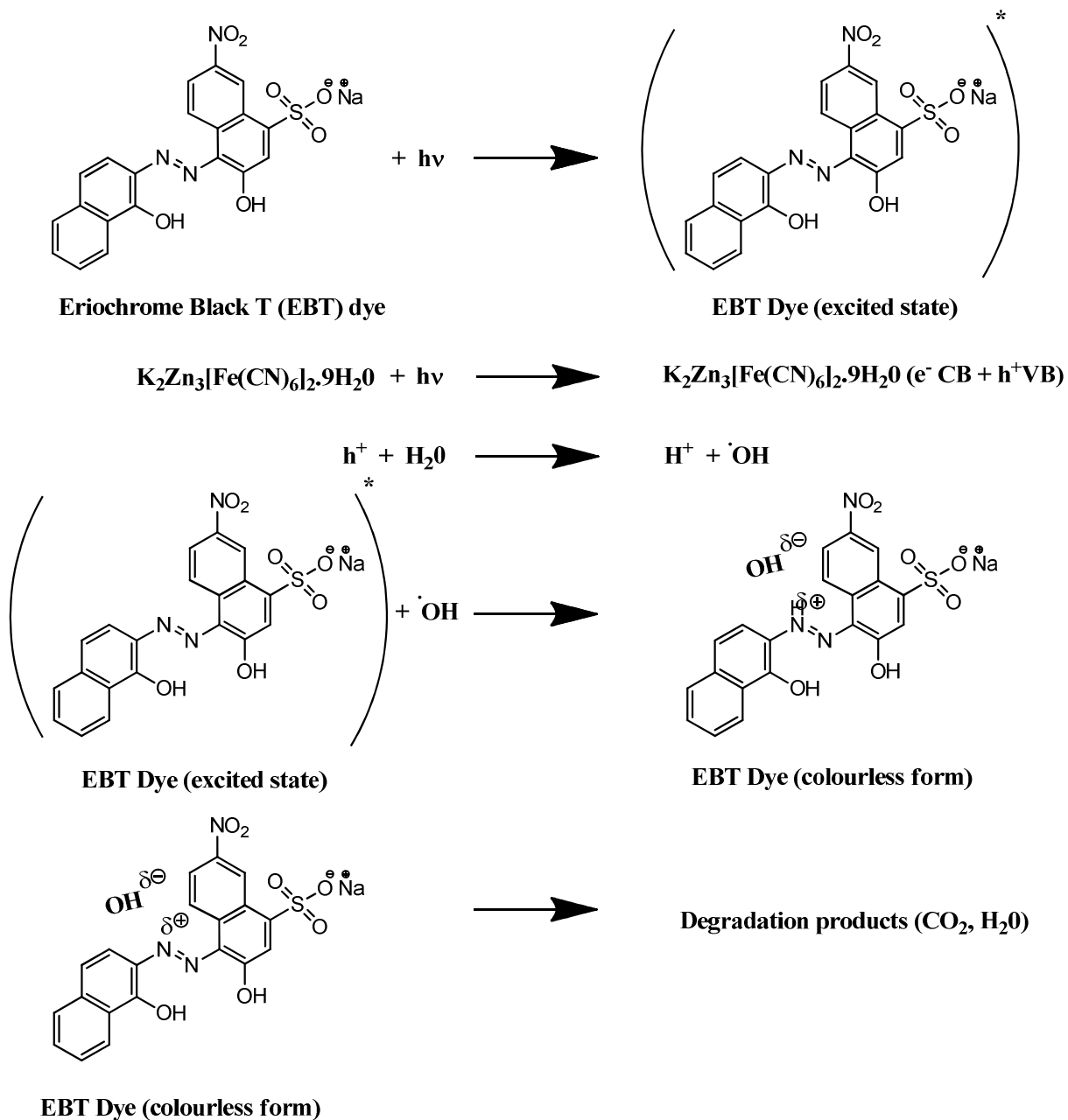


Figure 11: Photocatalytic degradation of EBT in presence of KZnHCF nanocubes

4. Conclusions

Monodisperse potassium zinc hexacyanoferrate nanocubes using *Sapindus Mukorossi* as a biosurfactant were synthesized through a novel green route. Synthesized nanocubes were evaluated as photocatalyst for the degradation of MG and EBT. Different process parameters like photocatalyst doze, initial dye concentration, pH and temperature were

studied in order to get the maximum dye degradation. MG was found to get degraded to the extent of 94.15% and EBT to 76.13% at pH, 7.0; ZnHCF, 15 mg; MG and EBT, 5ppm and temperature, ambient. Thus, the potassium zinc hexacyanoferrate nanocubes are the promising agents for the treatment of dyes contaminated industrial effluents.

- 5. Acknowledgement:** One of the authors Ms. Vidhisha Jassal is thankful to Ministry of Human Resource and Development (MHRD), New Delhi for providing financial assistance. Authors are also thankful to FIST-DST, New Delhi for providing the equipment (FT-IR and UV-VIS) used in characterization of the samples.

6. References:

1. De Tacconi, N. R., Rajeshwar, K., Lezna, R. O.: Metal hexacyanoferrates: electrosynthesis, in situ characterization, and applications. *Chem Mater.* 15, 3046–3062 (2003).
2. De Longchamp, D. M., Hammond, P. T.: Multiple-color electrochromism from layer-by-layer-assembled polyaniline/Prussian blue nanocomposite thin films. *Chem Mater.* 16, 4799–4805 (2004).
3. Kulesza, P. J., Malik, M. A., Miecznikowski, K., Wolkiewicz, A., Zamponi, S., Berrettoni, M., Marassi, R.: Counter cation sensitive electrochromism of cobalt hexacyanoferrate films. *J Electrochem Soc.* 143, 10–12 (1996).
4. De Tacconi, N. R., Rajeshwar, K., Lezna, R. O.: Preparation, photoelectro-chemical characterization, and photoelectrochromic behavior of metal hexacyanoferrate–titanium dioxide composite films. *Electrochim Acta.* 45, 3403–3411 (2000).
5. Wessells, C. D., McDowell, M. T., Peddada, S. V., Pasta, M., Huggins, R. A., Cui, Y.: Tunable reaction potentials in open framework nanoparticle battery electrodes for grid-scale energy storage. *ACS Nano.* 6, 1688–1694 (2012).
6. Torres-Gómez, G., Skaarup, S., West, K., Gómez-Romero, P.: Energy storage in hybrid organic–inorganic materials hexacyanoferrate-doped polypyrrole as cathode in reversible lithium cells. *J Electrochem Soc.* 147, 2513–2516 (2000).
7. Karyakin, A. A.: Prussian blue and its analogues: electrochemistry and analytical applications. *Electroanalysis.* 13, 813–819 (2001).
8. Eftekhari, A.: Electrochemical behavior and electrocatalytic activity of a zinc hexacyanoferrate film directly modified electrode. *J Electroanal Chem.* 537, 59–66 (2002).
9. James, J., Gomathi, H., Rao, G. P.: Modification of carbon electrodes with zinc hexacyanoferrate. *J Electroanal Chem.* 431, 231–235 (1997).
10. Sharma, O., Sharma, M. K.: Use of zinc hexacyanoferrate (ii) semiconductor in photocatalytic degradation of neutral red dye. *INTJCA.* 2, 1–13 (2013).
11. Maas, R., Chaudhari, S.: Adsorption and biological decolorization of azo dye reactive red 2 in semicontinuous anaerobic reactors. *Process Biochem.* 40, 699–705 (2005).

12. Chung, K. T., Stevens, S. Jr.: Decolourization of azo dyes by environmental microorganisms and helminthes. *Environ Toxicol Chem.* 12, 2121–2132 (1993).
13. Baldrian, P., Gabriel, J.: Lignocellulose degradation by *Pleurotus ostreatus* in the presence of cadmium. *FEMS. Microbiol Lett.* 220, 235–240 (2003).
14. Li, P., Song, Y., Wang, S., Tao, Z., Yu, S., Liu, Y.: Enhanced decolorization of methyl orange using zero-valent copper nanoparticles under assistance of hydrodynamic cavitation. *Ultrason Sonochem.* 22, 132–138 (2015).
15. Augugliaro, V., Bellardita, M., Loddo, V., Palmisano, G., Palmisano, L., Yurdakal, S.: Overview on oxidation mechanisms of organic compounds by TiO_2 in heterogeneous photocatalysis. *J Photochem Photobiol C.* 13, 224–245 (2012).
16. Sud, D., Kaur, P.: Heterogeneous Photocatalytic Degradation of Selected Organophosphate Pesticides: A Review. *Crit Rev Environ Sci Technol.* 42, 2365–2407 (2012).
17. Kumar, K. V., Sivanesan, S., Ramamurthi, V.: Adsorption of malachite green onto *Pithophora* sp. a fresh water algae: Equilibrium and kinetic modelling. *Process Biochem.* 40, 2865–2872 (2005).
18. Crini, G., Peindy, H. N., Gimbert, F., Robert, C.: Removal of C.I. basic green 4 (malachite green) from aqueous solutions by adsorption using cyclodextrin based adsorbent: Kinetic and equilibrium studies. *Sep Purif Technol.* 53, 97–110 (2007).
19. Srivastava, S., Sinha, R., Roy, D.: Toxicological effects of malachite green. *Aquat Toxicol.* 66, 319–329 (2004).
20. Arellano-Cárdenas, S., López-Cortez, S., Cornejo-Mazón, M., Mares-Gutiérrez, J. C.: Study of malachite green adsorption by organically modified clay using a batch method. *Appl Surf Sci.* 280, 74–78 (2013).
21. Ahmad, R., Kumar, R.: Adsorption studies of hazardous malachite green onto treat ginger waste. *J Environ Manage.* 91, 1032–1038 (2010).
22. Barka, N., Abdennouri, M., El-Makhfouk, M.: Removal of Methylene Blue and Eriochrome Black T from aqueous solutions by biosorption on *Scolymus hispanicus* L.: Kinetics, equilibrium and thermodynamics. *J Taiwan Inst Chem Eng.* 42, 320–326 (2011).

23. Baran, W., Makowski, A., Wardas, W.: The effect of UV radiation absorption of cationic and anionic dye solutions on their photocatalytic degradation in the presence TiO₂. *Dyes Pigments*. 76, 226–230 (2008).
24. Fiechter, A.: Biosurfactants: Moving towards industrial application. *Tibtech*. 10, 208-217 (1992).
25. Desai, J. D., Banat, I. M.: Microbial production of surfactants and their commercial potential. *Microbiol Mol Biol Rev*. 61, 47-64 (1997).
26. Dembitsky, M. V.: Astonishing diversity of natural surfactants: 1. Glycosides of fatty acids and alcohols. *Lipids*. 39, 933-953 (2004).
27. Mitra, S., Dungun, S.: Micellar properties of Quillaja saponin. Effects of temperature, salt and pH solution properties. *J Agric Food Chem*. 45, 1587-1595 (1997).
28. Berhow, M. A., Wagner, E. D., Vaughn, S. F., Plewa, M. J.: Characterization and antimutagenic activity of soybean saponins. *Mut Res*. 44, 11-22 (2000).
29. Shaker, K. H., Bernhardt, M., Elgamal, M. H. A., Seifert, K.: Triterpenoid saponins from *Fagonia indica*. *Phytochem*. 51, 1049-1053 (1999).
30. Mehta, P. S., Bhatt, K. C.: Traditional soap and detergent yielding plants of Uttaranchal. *Indian J Trad Knowl*. 6, 279-284 (2007).
31. Kommalpatti, R. R., Valsaraj, K. T., Constant, W. D., Roy, D.: Soil flushing using CGA suspensions generated from a plant-based surfactant. *J. Haz. Mat*. 60, 73-87 (1998).
32. Robber, J. M., Tyler, V. S.: *Pharmacognosy and pharmaco biotechnology*. pp. 1-14. Baltimore MD, Williams and Wilkins (1996).
33. Edeoga, H. O., Omosun, G., Uche, L. C.: Chemical composition of *Hyptis suaveolens* and *Ocimum gratissimum* hybrids from Nigeria. *Afri. J. Biotechnol*. 5, 892-895 (2006).
34. Cheeke, P. R.: Actual and potential applications of *Yucca schidigera* and *Quillaja saponaria* saponins in human and animal nutrition. In *proc. of the Amer. Soc. of Animal Sci*. 77, 1-10 (1999).
35. Urum, K., Pekdemir, T.: Evaluation of biosurfactant for crude oil contaminated soil washing. *Chemosphere*. 57, 1139-1150 (2004).

36. Chandra, K., Raj, D., Puri, S. P. Mossbauer studies of ferro and ferricyanide supercomplexes with 3D transition elements. *J. Phys. Chem.* 46, 1466 (1967).
37. Viladkar, S., Alam, T., Kamaluddin.: Adsorption of aromatic amines on metal ferrocyanides. *J Inorg Biochem.* 53, 69–78 (1994).
38. Wojdel, J. C and Bromley, S. T. Band gap variation in Prussian Blue via cation-induced structural distortion. *J. Phys. Chem. B* 110, 24294-24298 (2006).
39. Rosseinsky, D. R., Lim, H., Zhang, X., Jiang, H., Chai, J. W. Charge-transfer band shifts in iron(III) hexacyanoferrate(II) by electro-intercalated cations *via* ground state-energy/lattice-energy link. *Chem. Commun.* 24, 2988-2989 (2002).